



biblio.ugent.be

The UGent Institutional Repository is the electronic archiving and dissemination platform for all UGent research publications. Ghent University has implemented a mandate stipulating that all academic publications of UGent researchers should be deposited and archived in this repository. Except for items where current copyright restrictions apply, these papers are available in Open Access.

This item is the archived peer-reviewed author-version of: Disregarded Effect of Biological Fluids in siRNA Delivery: Human Ascites Fluid Severely Restricts Cellular Uptake of Nanoparticles

Authors: Dakwar G.R., Braeckmans K., Demeester J., Ceelen W., De Smedt S.C., Remaut K.

In: ACS Applied Materials & Interfaces 2015, 7(43): 24322-24329

To refer to or to cite this work, please use the citation to the published version:

Dakwar G.R., Braeckmans K., Demeester J., Ceelen W., De Smedt S.C., Remaut K. (2015) Disregarded Effect of Biological Fluids in siRNA Delivery: Human Ascites Fluid Severely Restricts Cellular Uptake of Nanoparticles. ACS Applied Materials & Interfaces 7 24322-24329

DOI: 10.1021/acsami.5b08805

Disregarded Effect of Biological Fluids in siRNA Delivery: Human Ascites Fluid Severely Restricts Cellular Uptake of Nanoparticles

George R. Dakwar^a, Kevin Braeckmans^{a,b}, Joseph Demeester^a, Wim Ceelen^c, Stefaan C. De Smedt^{a*} and Katrien Remaut^{a*†}

^a Laboratory for General Biochemistry and Physical Pharmacy, Ghent Research Group on Nanomedicines, Faculty of Pharmacy, Ghent University, Ottergemsesteenweg 460, 9000 Ghent, Belgium

^b Centre for Nano- and Biophotonics, Ghent University, 9000 Ghent, Belgium

^c Department of Surgery, Ghent University Hospital, De Pintelaan 185, 9000 Ghent, Belgium

* Equally contributed as senior author.

† Corresponding author. Tel.: +32 9 2648046; fax: +32 9 2648189

Keywords: liposomes, siRNA delivery, ascites, protein corona, lipofectamine, peritoneal metastasis

Abstract:

Small interfering RNA (siRNA) offers a great potential for the treatment of various diseases and disorders. Nevertheless, inefficient *in vivo* siRNA delivery hampers its translation into the clinic. While numerous successful *in vitro* siRNA delivery stories exist in reduced protein conditions, most studies so far overlook the influence of the biological fluids present in the *in vivo* environment. In this study, we compared transfection efficiency of liposomal formulations in Opti-MEM[®] (low protein content, routinely used for *in vitro* screening) and human undiluted ascites fluid obtained from a peritoneal carcinomatosis patient (high protein content, representing the *in vivo* situation). In Opti-MEM[®], all formulations are biologically active. In ascites fluid, however, the biological activity of all lipoplexes is lost, except for lipofectamine RNAiMAX[®]. The drop in transfection efficiency was not correlated to the physicochemical properties of the nanoparticles such as premature siRNA release and aggregation of the nanoparticles in the human ascites fluid. Remarkably, however, all the formulations, except for lipofectamine RNAiMAX[®], lost their ability to be taken up by cells following incubation in ascites fluid. To take into account the possible effects of a protein corona formed around the nanoparticles, we recommend to always use undiluted biological fluids for *in vitro* optimization of nano-sized siRNA formulations next to the conventional screening in low-protein content media. This should tighten the gap between *in vitro* and *in vivo* performance of nanoparticles, and ensure optimal selection of nanoparticles for further *in vivo* studies.

Introduction:

Since the discovery of small interfering RNA (siRNA)¹⁻², a lot of effort has been put in translating it into the clinic for the treatment of different diseases³. *In vitro* there are numerous options to successfully deliver siRNA to cells under ‘reduced serum conditions’. In more complex ‘protein-rich’ biological fluids, however, the effect of the protein corona (being formed at the surface of the nanoparticles) on the aggregation, release, uptake, intracellular trafficking and transfection of nanoparticles should not be underestimated⁴⁻⁶. Unfortunately, upon screening tens of papers which aim to optimize siRNA carriers for future *in vivo* use, the nanoparticles are only evaluated in unrealistic protein-free conditions, in spite of the fact that human biological fluids like e.g. blood, serum, plasma, ascites fluids, sputa, synovial fluids, ... are easily accessible. As these undiluted biological fluids contain high concentration of proteins, they more closely resemble the *in vivo* situation.

In vivo siRNA delivery is a complex process that includes both extracellular and intracellular barriers. Generally speaking, nanoparticles are expected to keep the cargo (i.e. siRNA) in an intact form while circulating in the biological fluids of the body. Also, pre-mature release of the siRNA from the nanoparticles and aggregation of siRNA nanoparticles in biological fluids are referred to as extracellular barriers for siRNA delivery⁷. While it is possible to determine the overall biological activity (i.e. gene knock down) of siRNA formulations *in vivo*, it is impossible to monitor siRNA release, aggregation and interaction of the formulations with biological membranes directly *in vivo*. Therefore, *in vitro* optimization of nanoparticle-based siRNA delivery is still needed, though should be done under conditions which are as similar as possible to the *in vivo* situation in which the nanoparticles are intended to be used.

A better understanding of our failure to efficiently deliver siRNA *in vivo*⁸ should arise from a stronger knowledge on the physico-chemical and biophysical properties of siRNA delivery systems in the biofluids which are expected to be encountered. For patients diagnosed with peritoneal carcinomatosis, for example, the delivery of nanoparticles in the peritoneal

cavity is being considered as a promising future therapy. Locoregional anticancer therapy allows to target the peritoneal carcinomatosis while at the same time limiting systemic toxicity. After locoregional administration, nanoparticles come into contact with the peritoneal fluid present in the peritoneal cavity of these patients. Hence, understanding the influence of peritoneal fluid on the performance of the nanoparticles is crucial. In the current study, we investigated the ability of different PEGylated and non-PEGylated cationic liposomes to induce siRNA knockdown in a human ovarian cancer cell line. We resembled the expected *in vivo* situation by incubating the nanoparticles in undiluted ascites fluid isolated from a peritoneal carcinomatosis patient. Important parameters of the liposomal formulations that we studied were i) the release of siRNA in the ascites fluid, ii) the aggregation of the lipoplexes and iii) the effect of the biofluid on the cellular uptake of nanoparticles. All parameters were correlated with the biological performance of the liposomal formulations. Our results indicate that there is a large discrepancy between the high transfection potential of the nanoparticles seen under protein-free conditions, and their performance which remains after exposing them to a protein-rich biofluid such as human ascites fluid.

Experimental section

Materials

(2,3-Dioleoyloxy-propyl)-trimethylammonium-chloride (DOTAP) and 1,2-Dioleoyl-sn-glycero-3-phosphoethanolamine (DOPE), and N-palmitoyl-sphingosine-1-{succinyl[methoxy(polyethylene glycol)2000]} (C16 mPEG 2000 Ceramide) were purchased from Avanti Polar Lipids (Alabaster, AL, USA). Chloroform, 4-(2-hydroxyethyl)-1-piperazineethanesulfonic acid (HEPES), 3-(4,5-Dimethyl-2-thiazolyl)-2,5-diphenyl-2H-tetrazolium bromide (MTT) and sodium chloride (NaCl) were purchased from Sigma Aldrich (Bornem, Belgium).

Penicillin-Streptomycin (5000 U/ml), Lipofectamine[®] RNAiMAX Transfection Reagent (LF), L-Glutamine (200 mM), 0.25% Trypsin-EDTA (1X) Phenol Red, McCoy's 5A (Modified), Opti-MEM[®] and 1,1'-dioctadecyl-3,3,3',3'-tetramethylindodicarbocyanine perchlorate (DID) (λ_{ex} = 644 nm, λ_{em} = 665 nm) were purchased from Invitrogen (Merelbeke, Belgium). Luciferase Assay Substrate was purchased from Promega (Madison, WI, USA). Fetal Bovine Serum (FBS) was purchased from HyClone[®] Thermo Scientific (Cramlington, UK). Passive Lysis Buffer and Luciferase Assay Kit were purchased from (Promega, Leiden, Netherlands). Negative control siRNA (siNEG) and Luciferase siRNA (siLuc) were purchased from (Eurogentec, Searing, Belgium).

Preparation and characterization of the lipoplexes (LPXs)

Liposomes corresponding to 5 mM of DOTAP and 5 mM of DOPE lipids were prepared by mixing the appropriate amount of lipids in a round bottomed flask before evaporation. PEGylated liposomes were prepared by adding the desired amounts of C16 Cer-PEG dissolved in chloroform (corresponding to 5 mol%) to the lipids before evaporation. A lipid film was formed by rotary evaporation of the chloroform at 40°C. Liposomes were prepared by rehydrating the lipid film with HEPES buffer (20 mM, pH 7.4), followed by sonication using a probe sonicator (Branson Ultrasonics Digital Sonifier[®], Danbury, USA). LPXs of +/- charge

ratio of 8 were prepared by adding appropriate amounts of liposomes to siRNA. The mixture was incubated at room temperature to allow formation of the LPXs. Lipofectamine RNAiMAX[®] LPXs were prepared as described by the manufacturer. Briefly, appropriate volume of Lipofectamine RNAiMAX[®] was added to a solution of respectively siNEG, siLuc or fluorescently labeled siRNA and incubated at room temperature for 15 minutes before use. Throughout the manuscript Lipofectamine RNAiMAX[®] lipoplexes will be termed LF-LPXs.

The average size and zeta potential of all formulations were measured by a Zetasizer Nano-ZS (Malvern, Worcestershire, UK).

Cell culture

The human ovarian cancer cell line SKOV-3 which stably expresses firefly luciferase was used for *in vitro* experiments. Cells were cultured in McCoy's 5A medium supplemented with FBS, Penicillin-Streptomycin. Cells were cultured until 80% to 90% confluency and detached from tissue culture dishes with 0.25% trypsin. Cells were maintained in an incubator at 37°C in a humidified atmosphere with 5% CO₂.

Transfection efficiency

SKOV-3 cells were cultured overnight on 24-well plates (35,000 cells/well) in 500 µl of medium containing 10% FBS. Then, cells were washed and incubated with the LPXs and LF-LPXs in Opti-MEM[®] during 4 h. After 4 h of incubation, the transfection medium was replaced by culture medium and cells were returned to the incubator for 24 h. The siLuc concentration in the wells equaled 25 nM. LF-LPXs, prepared as recommended by the manufacturer, were used as positive control. Each LPX containing siLuc was compared with its own control (e.g. siNEG).

After overnight incubation, cells were lysed with Passive Lysis Buffer and analyzed for firefly luciferase expression using the luciferase assay kit (Promega). The bioluminescence (Relative

Light Units, RLU) was measured using a GloMax Luminometer (Promega). The percentage of luciferase down regulation was determined by the following equation:

% transfection = $100 - (100 \times \text{RLU}_{\text{Luc}}/\text{RLU}_{\text{NEG}})$, where RLU_{NEG} and RLU_{Luc} are the mean bioluminescence as measured for respectively siNEG and siLuc. The data shown in Figure 2 is based on 3 experiments performed on 3 different days.

For transfections in the ascites fluid, 300 μl LPXs (of each formulation) were first added to 700 μl ascites fluid and incubated for 1 h. Then, 300 μl of this mixture was added to 700 μl of Opti-MEM[®] in each well of a 24 well-plate. Thereafter, the medium was replaced with growth medium and cells were returned to the incubator for 24 h as described above.

So named ‘upside-down transfections’ were performed as follows: 300 μl LF-LPXs were incubated for 1 and 3 h at 37°C in 700 μl of human ascites fluid . SKOV-3 cells were cultured (during 24h) on 12 mm coverslips. Subsequently the cells (on the coverslips) were mounted upside-down on plastic tubes (diameter 1.3 cm, height 0.9 cm), filled with 700 μl Opti-MEM[®]. Then, 300 μl LF-LPXs were added to these tubes as such or after incubation in the ascites fluid. After 4 h of exposing the LF-LPXs to the cells, the coverslips were placed in the wells of a 24-well plate and kept in the incubator for 24 h after adding growth medium to the cells. Subsequently the cells were lysed and the percentage of luciferase inhibition was calculated as mentioned above. It should be noted that in this upside-down transfection mode, precipitation of LF-LPXs on the cells due to gravity is avoided.

Statistical analysis (shown in Figure 1.) was performed using GraphPad Prism 6 (GraphPad[®], USA). Statistically significant differences were calculated by using an analysis of variance (ANOVA) at a 0.05 significance level, followed by Sidak’s post test. For each formulation, transfection experiment carried-out in Opti-MEM[®] were compared to those in ascites.

Fluorescence Correlation Spectroscopy on LPXs

Fluorescence Correlation Spectroscopy (FCS) is a microscopy-based technique that monitors the fluorescence intensity fluctuations of (fluorescent) molecules diffusing in and out of the focal volume of a confocal microscope^{7, 10}. Single color FCS measurements were performed on LPXs containing 30% Cy5 siRNA, with a +/- charge ratio of 8. Five μ l of such LPXs was diluted to a final volume of 45 μ l HEPES buffer or 45 μ l ascites fluid (~ 90 vol% of biofluid); The samples were analysed by FCS immediately, 1 h and 24 h after incubation in the biofluids at 37°C. During the incubation and FCS measurements, the well plate was covered with Adhesive Plates Seals (Thermo Scientific, UK) to avoid evaporation of the sample and to minimize flow. FCS measurements were performed on the experimental set-up described before⁷.

Fluorescence single particle tracking (fSPT)

Fluorescence single particle tracking (fSPT) is a fluorescence microscopy technique which is very well suited to determine diffusion/aggregation of nanoparticles in undiluted biological fluids, as was previously shown¹¹.

fSPT measurements were performed on LPXs (Cationic, 5% C16 Cer-PEG and LF-LPXs), labeled with DID or containing Alexa-Fluor 488 (AF-488) labeled siRNA. LPXs were dispersed in biofluids as follows. First, formulations were diluted 400 times in HEPES buffer. Then 5 μ l was added to 45 μ l of human ascites fluid (~ 90 vol% of biofluid), and incubated for respectively 1, 2 and 3 h at 37°C in a 96-well plate (Greiner bio-one, Frickenhausen, Germany). At the end of the incubation time, the samples were placed on a custom-built fSPT set-up¹¹ and movies were recorded at about 5 μ m above the bottom of the 96-well plate. Videos were analyzed as was previously explained using the following values of viscosity at room temperature: 1.39 cP for the ascites fluid and 0.94 cP for HEPES buffer⁷. Human ascites fluid was obtained from a patient diagnosed with peritoneal carcinomatosis at the medical oncology

department of Ghent University hospital (approved by the ethics committee of the Ghent University hospital (# 2013/589)).

Internalization of siRNA into SKOV-3 cells

SKOV-3 cells were plated on 24-well plates (35,000 cells in each well) and allowed to grow in an incubator for 24 h. For uptake experiments, cells were incubated in Opti-MEM[®] with fluorescent LPXs containing 10% of AF-488 siRNA for 4 h at 37°C and 4°C. At the end of the incubation, cells were washed extensively with warm growth medium and PBS, then detached using trypsin and analyzed by FACS (FACSCalibur Flow Cytometer, BD Biosciences, USA). Uptake experiments were performed with LPXs as such (directly after preparation), or after incubation of the LPXs with ~70% ascites fluid for 1 h before adding them to the cells, as described above under transfection efficiency.

Results

Characterization of the liposomes and LPXs in HEPES buffer

As depicted in **table 1**, all the formulations resulted in nano-sized vesicles, as determined by dynamic light scattering (DLS). Despite of the fact that the average size of the LF based liposomes (LF-LP) and LF lipoplexes (LF-LPXs) were in the same range as the other formulations, the polydispersity of the LF-LP and LF-LPXs was higher (polydispersity index (PDI) > 0.5). The size increased for all formulations upon complexation of the liposomes with siRNA (except for LF-LPXs).

The cationic liposomes and LPXs showed the highest positive surface charge (as reflected from their zeta-potential). As expected, PEGylation lowered the surface charge of the liposomes and the LPXs. LF-LP and LF-LPXs showed an intermediate surface charge.

Transfection efficiency of the LPXs in protein-free and protein-rich conditions

To evaluate the ability of the LPXs to knockdown the expression of a specific gene, SKOV-3 cells stably expressing luciferase were incubated with the LPXs containing siRNA against luciferase (siLuc). To verify the knockdown specificity, formulations loaded with a scrambled sequence (siNEG) were used as well.

Figure 1 (dark grey bars) demonstrates the transfection efficiency of the LPXs following incubation in Opti-MEM[®]. All the formulations efficiently down regulated luciferase expression.

Considering the fact that nanoparticles for *in vivo* intraperitoneal gene therapy will come into contact with peritoneal fluids, we were interested to see whether incubation of the LPXs in the ascites fluid obtained from a human peritoneal carcinomatosis patient would influence their transfection efficiency. The white bars in Figure 1 show a dramatic significant decrease in the transfection efficiency for the cationic LPXs and 5% C16 Cer-LPXs, while the LF-LPXs remain active. This raised the question as to why the LPXs and 5% C16 Cer-LPXs significantly lost their biological activity upon exposure to human ascites fluid.

Release of siRNA from LPXs in undiluted human ascites fluid

A possible reason why LPXs are less efficient in human ascites fluid could be a premature release of siRNA from the formulations. Indeed, the more siRNA is released from the carriers, the less siRNA remains available for uptake in cells. As demonstrated previously by us, FCS is a suitable method to determine the amount of siRNA that is present in nanocarriers⁹⁻¹⁰. Likewise, FCS can be used to follow the release of siRNA from nanoparticles upon incubating them in buffer and biological fluids⁷.

Figure 2 shows the percentage of siRNA that is associated with the different formulations in HEPES buffer immediately following preparation (e.g. complexation efficiency) and after incubation for 1 h and 24 h in human ascites fluid (90% vol). In HEPES buffer (grey bars), cationic LPXs show the highest complexation efficiency, with more than 90% of the siRNA associated to the cationic liposomes. PEGylation of the cationic liposomes seems to reduce the complexation efficiency as only 75% of the siRNA is bound to the 5% C16-Cer LPXs. LF-LPXs have the lowest loading efficiency with 65% of siRNA complexed .

Following 1 h of incubation in human ascites fluid (white bars), all formulations release a substantial amount of the initially complexed siRNA, leaving only 50%, 40% and 40% of siRNA complexed in cationic LPX, 5% C16-Cer LPXs and LF-LPXs ,respectively. Following 24 h of incubation in human ascites fluid, release of siRNA continues, resulting in less than 20% of siRNA remaining complexed in all the formulations (dark grey bars). Taken together, human ascites fluid induces a massive release of siRNA from all liposomal formulations, reducing the amount of complexed siRNA that remains available for biological activity to about 20%.

The substantial loss of siRNA following incubation in ascites fluid could explain the lower transfection efficiency of the cationic LPXs and 5% C16 Cer-LPXs in Figure 1. Nevertheless,

also LF-LPXs retain only 20% of complexed siRNA, while maintaining their biological activity. In a next step, we evaluated the aggregation of the complexes in the undiluted human ascites fluids and whether or not this aggregation influences the biological activity of the complexes.

Aggregation of the LPXs in undiluted human ascites fluid

In our previous study⁷, we have shown that dynamic light scattering (DLS) is not an ideal technique for quantifying the extent of aggregation of nanocarriers in (undiluted) ascites fluids, simply due to light scattering that results from the high amount of proteins in such samples. In our hands fSPT has proven to be superior over DLS to study aggregation of nanoparticles in biological fluids^{7, 11-13}. Figure 3a shows the size distributions of the cationic LPXs incubated in undiluted human ascites fluid (~ 90 vol% of biofluid) during 1, 2 and 3 h. In HEPES buffer the average diameter of the cationic LPXs is about 200 nm. In ascites fluid aggregation in time clearly occurs with the formation of 1-2 μm sized aggregates. 5% C16 Cer-LPXs have an average size of 150 nm in HEPES buffer (Figure 3b, black curve). Following 1 h of incubation in ascites fluid, the size distribution is (very) slightly shifted towards the right showing aggregation of a specific population of particles, particularly those that were initially smaller than 100 nm (Figure 3b, red curve). After 2 h of incubation, aggregation seems to become more outspoken, with an average diameter of 200 nm (Figure 4b, blue curve). No further aggregation was observed following 3 h of incubation (Figure 4b, green curve). Figure 3b confirms our previous results that PEGylation protects liposomes from aggregation in undiluted human ascites fluid⁷.

LF-LPXs showed a high polydispersity in HEPES buffer, with particles ranging from tens of nanometers up to 1 μm in size (Figure 3c, black curve). Following incubation in ascites fluid we observed a slight aggregation after 1 h of incubation (Figure 4c, red curve), followed by a

pronounced aggregation after 2 and 3 h (Figure 3c, green and blue curve), with the presence of micron-sized particles.

Based on the data in Figure 4c, it is clear that very severe aggregation occurs in ascites fluids for LF-LPXs. Figure 1 demonstrates that LF-LPXs exposed to ascites fluids show the highest transfection efficiency, while the (more) colloiddally stable cationic LPXs and 5% C16 Cer-LPXs lose their biological activity in ascites fluid (Figure 1, white bars). One possible reason for these observations could be that the larger LF-LPXs aggregates rapidly sediment onto the cells during transfection, leading to a forced increased uptake and transfection efficiency. To test this hypothesis, the cell uptake of the lipoplexes was evaluated before and after incubation of the formulations in ascites fluid.

Influence of ascites fluid on the cellular uptake of the LPXs by SKOV-3 cells

To test the extent of LPX uptake in cells after incubation with ascites fluid, we exposed SKOV-3 cells to LPXs loaded with fluorescently labeled AF-488 siRNA and quantified their uptake by flow cytometry. Figure 4a indicates that in Opti-MEM[®] (and at 37°C) the various types of LPXs carried the fluorescent siRNA into SKOV-3 cells. At 4°C, intracellular AF-488 fluorescence was minimal (data not shown), indicating that at 37°C the LPXs were indeed internalized and did not just attach at the surface of the cells. When the same experiment was performed with LPXs that were incubated in ascites fluid for 1 h, the cationic LPXs and the 5% C16 Cer-LPXs completely lost their ability to carry the fluorescent siRNA into the cells, as depicted in Figure 4b. Only LF-LPXs were still efficiently internalized into SKOV-3 cells.

Aggregation is not the sole determinant of *in vitro* transfection efficiency

As Figure 3c demonstrates that mainly LF-LPXs form large aggregates in ascites fluid, which may easily sediment on the cells, we wondered whether those severe aggregates explain why LF-LPXs keep transfecting the cells. Therefore, we tested the ability of LF-LPXs to transfect SKOV-3 cells in an “upside-down transfection mode” where cells are positioned at the top surface of the LPXs dispersions, thus avoiding the spontaneous sedimentation of aggregates on the cells. Upside-down transfections were performed with LF-LPXs in Opti-MEM[®] and with LF-LPXs that were incubated in ascites fluid during 1 or 3 h. As depicted in Figure 5, in Opti-MEM[®] luciferase down regulation remained 80%, which is similar as in the ‘normal transfection mode’ (see Figure 1). This demonstrates that in Opti-MEM[®], LF-LPXs can equally well transfect cells which are below (Figure 1) or on top (Figure 5) of the LF-LPX solution, thereby ruling out the possibility that only aggregates contribute to the transfection efficiency. Following incubation of LF-LPXs for 1 h and 3 h in the ascites fluid, the transfection efficiency decreased to 40% in the upside-down transfection mode (Figure 5), while this decrease was not observed in the ‘normal transfection mode’ (see Figure 1). Our data suggest that in the ‘upside-down transfection mode’, the non-aggregated fraction of the LF-LPXs can reach 40% of the cells, while in the ‘normal transfection mode’ an additional 40% of cells are transfected by LF-LPXs aggregates that are formed in ascites fluid and sediment onto the cells. Therefore, aggregates can indeed contribute to the transfection efficiency, though they are not solely responsible for the observed biological activity.

Discussion

siRNA mediated downregulation of disease related proteins is a very promising therapeutic application. Although numerous efficient nanoparticles have been identified for successful siRNA delivery *in vitro*, the actual number of formulations that withstand the harsh *in vivo* conditions is extremely disappointing. *In vivo*, nanoparticles face additional barriers such as protein-rich biofluids which are not present in the widely used protein-free conditions when screening nanoparticles *in vitro*. Hence, the influence of extracellular fluids on the nanoparticles performance after administration to the human body is often overlooked. In this study, we evaluated the potential of non-PEGylated and PEGylated liposomal formulations to successfully deliver siRNA to a human ovarian cancer cell line. Considering the potential use of locoregional administration of lipid-based siRNA carriers to treat peritoneal metastasis, nanoparticles in this study were tested in human ascites fluid, obtained from a carcinomatosis patient. Additionally, biological activity was determined in the widespread used low-protein content medium Opti-MEM[®]. Importantly, solely based on transfections in this low-protein medium, all formulations performed up to expectations. Unfortunately, when incubating the formulations in a high-protein content medium (i.e. ascites fluid in this study), only LF-LPXs were able to keep their original efficiency. To explain the drop in transfection efficiency, we evaluated three important properties of the nanoparticles, namely premature siRNA release, nanoparticle aggregation and cellular uptake in the presence of human ascites fluid.

Complexation of siRNA to (cationic) carriers is necessary to enhance the cellular uptake of these negatively charged nucleic acids. Hence, premature release of siRNA from the nanocarriers in the biofluids, before cellular uptake has taken place, will result in a lower amount of siRNA that is able to reach the cytoplasm of the cells. Using Fluorescence Correlation Spectroscopy, we found that all tested formulations showed release of siRNA in the presence of ascites fluid. This siRNA release most likely results from competition between siRNA and the abundantly present negatively charged proteins in the human ascites fluid for

binding to the positively charged liposomes. Although testing release of siRNA in protein-rich conditions can tell us something about the fraction of siRNA that is lost, it is important to note that the absolute values of complexed siRNA were not predictive for the expected biological activity. Indeed, all formulations end up with almost the same amount of remaining siRNA following 24 h of incubation (Figure 2), while clear differences in transfection efficiency exist (Figure 1).

As the uptake of nanoparticles is both charge and size dependent, aggregation of nanoparticles can potentially influence the uptake profile and subsequent transfection efficiency¹⁴. Therefore, we evaluated if aggregation of the nanoparticles was related to the obtained biological activity. On the contrary to the release profile, the differences in aggregation between the formulations is much more pronounced. Aggregation is most pronounced in the case of the cationic LPXs, while in the case of C16 Cer-LPXs the PEG chains protect the LPXs from aggregation. One could argue that the formation of large aggregates could be the reason why lipofectamine RNAiMAX[®] is still efficiently transfecting cells after incubation in ascites fluid. Indeed, aggregates are expected to sediment onto cells and in this way, a larger amount of nanoparticles (and thus concentration of siRNA) comes into contact with cells during the 4 hours incubation period. When ruling out this sedimentation with an upside-down transfection setup, however, LF-LPXs still retained 50% of their transfection efficiency, demonstrating that aggregation alone cannot be the sole reason for the better transfection efficiency of LF-LPXs. Aggregation of particles remains however extremely important for the *in vivo* situation, as large aggregates can cause severe toxicity such as blocking the blood capillaries. Therefore, aggregation studies remain predictive of the suitability of nanoparticles for the *in vivo* situation and one should keep in mind that strongly aggregated nanoparticles have no future for *in vivo* use, even when high *in vitro* transfection efficiencies were obtained.

Cellular uptake is a first important step of the intracellular journey of nanoparticles. Importantly, the drop in the transfection of the cationic and PEGylated LPXs does correspond with the observation that the complexes are no longer internalized into cells after incubation in ascites fluid (Figure 4b). As we measure the uptake based on fluorescent siRNA, a pre-mature release of siRNA in the ascites fluid would lower the amount of complexed siRNA that can enter the cells and be detected. The amount of released siRNA in ascites fluid is however comparable for the three formulations studied (Figure 2). As all formulations contained at least still 40% of complexed siRNA, the possible internalization of the complexes should be detectable. The fact that only LF-LPXs are still taken up in the cells after pre-incubation in ascites fluid could in theory also be ascribed to the sedimentation of a larger amount of particles onto the cells. As described above, however, LF-LPXs also transfect (and thus are taken up) in an upside down transfection setup to which larger aggregates do not contribute.

When nanoparticles are dispersed in extracellular fluids, proteins in these biofluids may bind at the surface of the nanoparticles, forming a so-called protein corona. It has been shown that the protein corona formed around transferrin-functionalized nanoparticles impairs their ability to bind transferrin receptors on the cell surface following incubation in fetal bovine serum and human serum¹⁵⁻¹⁶. Also, the protein corona can alter the intracellular processing of particles, increasing the fraction that accumulates in the lysosomes¹⁷. Both the protein composition of the biofluid and the surface properties of the nanoparticles will determine the composition of the protein corona that is eventually formed. We have previously shown that the protein concentration in human ascites fluid is half the concentration of proteins present in human serum, while the protein composition of human ascites fluid is very similar to human serum, with albumin as main fraction (62%)⁷. We hypothesize that the poor uptake observed following incubation of cationic LPXs and PEGylated LPXs in the ascites fluid results from the surface coating of these formulations with negatively charged proteins¹⁸. It is worth mentioning that

this is not the first study showing that nanoparticles lose their ability to interact with biological membranes following incubation with a protein-rich biological environment. Interestingly, very recently also Hadjidemetriou et al. reported that bare and PEGylated liposomes significantly lost their ability to internalize into cells following incubation in undiluted plasma¹⁹. This points out that the detrimental effect of human ascites fluid on the internalization of nanoparticles could be a common problem for many nanoparticle formulations exposed to various biological fluids. As for nucleic acid delivery, uptake is necessary for biological activity, testing the uptake of gene delivery systems following incubation in undiluted biological fluids is extremely important and should become a routine test before performing *in vivo* studies. Taken together, the “protein corona field” is rapidly growing with new findings that are extremely important for translating the *in vitro* to the *in vivo* situation, but is still not getting enough attention among scientists in the RNAi delivery community.

Conclusions

Importantly, we found that good complexation and transfection properties in reduced serum conditions like Opti-MEM[®] are not predictive to the actual performance of nanoparticles after being exposed to more complex biological fluids such as human ascites fluid. Based on our results the most important factor that eventually determines the biological activity is the biological fluid in which the particles are incubated with prior to adding them on cells. The composition of the biological fluid may substantially influence the extent of release, aggregation, uptake and biological activity of nano-sized siRNA formulations. Therefore, we strongly recommend to perform *in vitro* optimization of nano-sized siRNA formulations in undiluted biological fluids taking into account the route of administration, regardless of the type of the formulation (lipid-based or polymer-based), before assessing the transfection efficiency of nanoparticles *in vivo*. As most biofluids such as peritoneal fluid in the case of intraperitoneal

gene delivery and serum or blood in the case of intravenous (IV) delivery are relatively easily accessible, testing nanoparticles in these more complex biological environments is very feasible and far more representative for the *in vivo* situation. Based on assays performed in protein free (Opti-MEM[®]) conditions only, one runs the risk to select nanoparticles that are able to cross an empty street, hoping they will also survive the busy traffic conditions *in vivo*. Just like earning a driving license, however, nanoparticles should be tested in realistic *in vitro* conditions so that *in vivo* animal testing can be restricted to only those particles that passed the relevant screening conditions.

Associated Content

Supporting Information Available: average diameter of the studied LPXs following 3 h of incubation in ascites fluid

Author information

Corresponding author

E-mail: Katrien.Remaut@ugent.be (K. Remaut)

Author Contributions :

†K. Remaut and S. De Smedt contributed equally to this work.

Notes:

The authors declare no competing financial interest.

Acknowledgments

This research was supported by the Research Foundation-Flanders (FWO) (grant No. G006714N) for K.R., J.D., S.D.,W.C. and the BOF – Special Research Fund of the Ghent University (grant No. 01B01108) for K.B. S.D.

We thank Senne Cornelis for his help with the experiments.

References

1. Elbashir, S. M.; Harborth, J.; Lendeckel, W.; Yalcin, A.; Weber, K.; Tuschl, T., Duplexes of 21-Nucleotide RNAs mediate RNA Interference in Cultured Mammalian Cells. *Nature*. **2001**, *6836*, 494-498.
2. Fire, A.; Xu, S. Q.; Montgomery, M. K.; Kostas, S. A.; Driver, S. E.; Mello, C. C., Potent and specific Genetic Interference by Double-Stranded RNA in *Caenorhabditis Elegans*. *Nature*. **1998**, *6669*, 806-811.
3. Lares, M. R.; Rossi, J. J.; Ouellet, D. L., RNAi and Small Interfering RNAs in Human Disease Therapeutic Applications. *Trends. Biotechnol.* **2010**, *11*, 570-579.
4. Dell'Orco, D.; Lundqvist, M.; Linse, S.; Cedervall, T., Mathematical Modeling of the Protein Corona: Implications for Nanoparticulate Delivery Systems. *Nanomed-UK*. **2014**, *6*, 851-858.
5. Fleischer, C. C.; Payne, C. K., Nanoparticle-Cell Interactions: Molecular Structure of the Protein Corona and Cellular Outcomes. *Acc. Chem. Res.* **2014**, *8*, 2651-2659.
6. Walkey, C. D.; Chan, W. C. W., Understanding and Controlling the Interaction of Nanomaterials with Proteins in a Physiological Environment. *Chem. Soc. Rev.* **2012**, *7*, 2780-2799.
7. Dakwar, G. R.; Zagato, E.; Delanghe, J.; Hobel, S.; Aigner, A.; Denys, H.; Braeckmans, K.; Ceelen, W.; De Smedt, F. C.; Remaut, K., Colloidal Stability of Nano-Sized Particles in the Peritoneal Fluid: Towards Optimizing Drug Delivery Systems for Intraperitoneal Therapy. *Acta. Biomater.* **2014**, *7*, 2965-2975.
8. Conde, J.; Artzi, N., Are RNAi and miRNA Therapeutics Truly Dead? *Trends. Biotechnol.* **2015**, *3*, 141-144.
9. Buyens, K.; Demeester, J.; De Smedt, S. C.; Sanders, N. N., Elucidating the Encapsulation of Short Interfering RNA in PEGylated Cationic Liposomes. *Langmuir.* **2009**, *9*, 4886-4891.
10. Buyens, K.; Lucas, B.; Raemdonck, K.; Braeckmans, K.; Vercammen, J.; Hendrix, J.; Engelborghs, Y.; De Smedt, S. C.; Sanders, N. N., A Fast and Sensitive Method for Measuring the Integrity of siRNA-Carrier Complexes in Full Human Serum. *J. Control. Release.* **2008**, *1*, 67-76.

11. Braeckmans, K.; Buyens, K.; Bouquet, W.; Vervaet, C.; Joye, P.; De Vos, F.; Plawinski, L.; Doevre, L.; Angles-Cano, E.; Sanders, N. N.; Demeester, J.; De Smedt, S. C., Sizing Nanomatter in Biological Fluids by Fluorescence Single Particle Tracking. *Nano. Lett.* **2010**, *11*, 4435-4442.
12. Naeye, B.; Deschout, H.; Caveliers, V.; Descamps, B.; Braeckmans, K.; Vanhove, C.; Demeester, J.; Lahoutte, T.; De Smedt, S. C.; Raemdonck, K., In vivo Disassembly of IV Administered siRNA Matrix Nanoparticles at the Renal Filtration Barrier. *Biomater.* **2013**, *9*, 2350-2358.
13. Naeye, B.; Deschout, H.; Roding, M.; Rudemo, M.; Delanghe, J.; Devreese, K.; Demeester, J.; Braeckmans, K.; De Smedt, S. C.; Raemdonck, K., Hemocompatibility of siRNA Loaded Dextran Nanogels. *Biomater.* **2011**, *34*, 9120-9127.
14. Rejman, J.; Oberle, V.; Zuhorn, I. S.; Hoekstra, D., Size-Dependent Internalization of Particles via the Pathways of Clathrin-and Caveolae-Mediated Endocytosis. *Biochem. J.* **2004**, *377*, 159-169.
15. Caracciolo, G., Liposome-Protein Corona in a Physiological Environment: Challenges and Opportunities for Targeted Delivery of Nanomedicines. *Nanomed. Nanotechnol. Biol. Med.* **2015**, *3*, 543-557.
16. Salvati, A.; Pitek, A. S.; Monopoli, M. P.; Prapainop, K.; Bombelli, F. B.; Hristov, D. R.; Kelly, P. M.; Aberg, C.; Mahon, E.; Dawson, K. A., Transferrin-Functionalized Nanoparticles Lose their Targeting capabilities when a Biomolecule Corona Adsorbs on the Surface. *Nat. Nanotechnol.* **2013**, *2*, 137-143.
17. Wang, F. J.; Yu, L.; Monopoli, M. P.; Sandin, P.; Mahon, E.; Salvati, A.; Dawson, K. A., The Biomolecular Corona is Retained during Nanoparticle Uptake and Protects the Cells from the Damage Induced by Cationic Nanoparticles until Degraded in the Lysosomes. *Nanomed. Nanotechnol. Biol. Med.* **2013**, *8*, 1159-1168.
18. Fleischer, C. C.; Payne, C. K., Nanoparticle-Cell Interactions: Molecular Structure of the Protein Corona and Cellular Outcomes. *Acc. Chem. Res.* **2014**, *8*, 2651-2659.
19. Hadjidemetriou, M.; Al-Ahmady, Z.; Mazza, M.; Collins, R. F.; Dawson, K.; Kostarelos, K., In Vivo Biomolecule Corona around Blood-Circulating, Clinically Used and Antibody-Targeted Lipid Bilayer Nanoscale Vesicles. *ACS Nano* **2015**, *8*, 8142-8156.

Tables

Table 1.

Z-Average diameter and zeta potential of the different formulations used in this study

Formulation		Z-Average diameter \pm SD (nm)	Polydispersity index (PDI)	Zeta-potential (mV) (mean \pm SD)	Abbreviation
Cationic	Liposomes	85 \pm 1	0.2	56 \pm 1	Cationic LP
	LPX	107 \pm 1	0.2	53 \pm 1	Cationic LPXs
5% C16 Cer-PEG	Liposomes	115 \pm 2	0.2	6 \pm 1	5% C16 Cer-LP
	LPX	151 \pm 2	0.2	5 \pm 1	5% C16 Cer-LPXs
Lipofectamine RNAiMAX [®]	Liposomes	137 \pm 12	0.6	26 \pm 2	LF-LP
	LPX	106 \pm 3	0.6	22 \pm 3	LF-LPXs

Legends

Figure 1

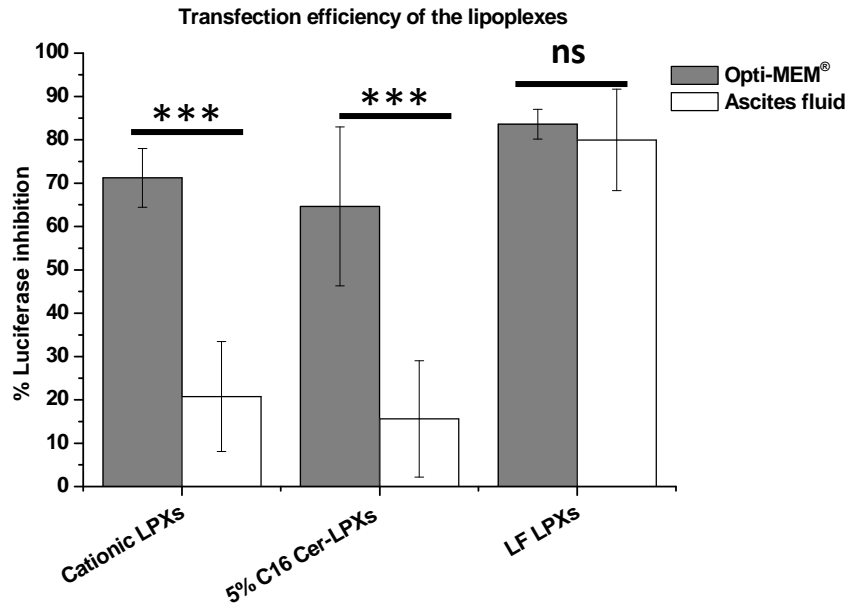


Figure 1. Inhibition of luciferase in SKOV-3 cells by the lipoplexes in Opti-MEM® (dark grey bars) and following incubation of the lipoplexes for 1 h in ascites fluid (70 vol%) (white bars). The values in the graph represent the average from at least 3 experiments that were performed on different days.

Figure 2

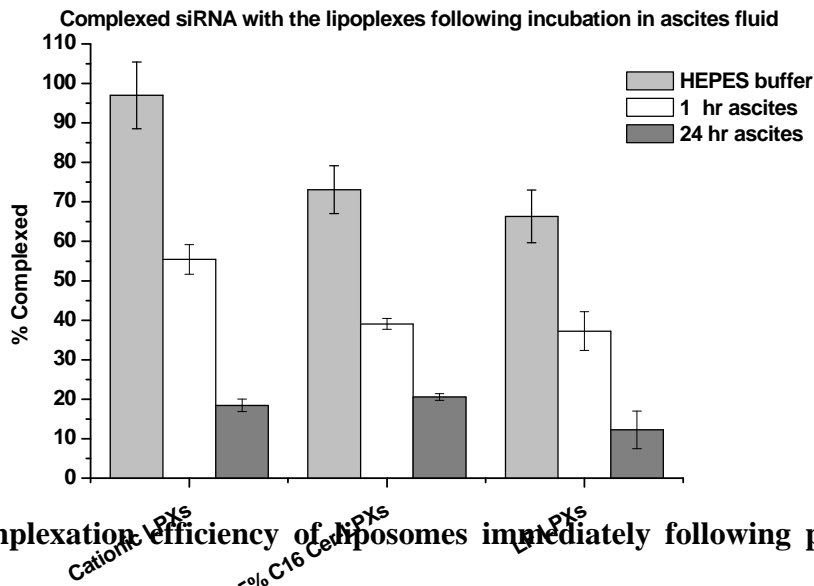
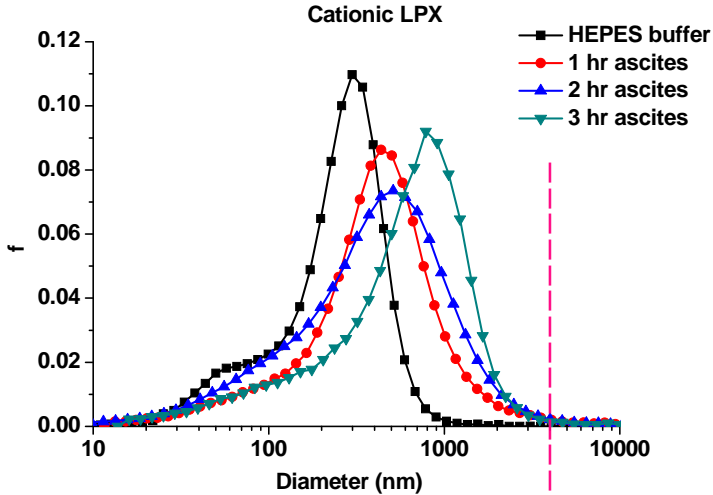


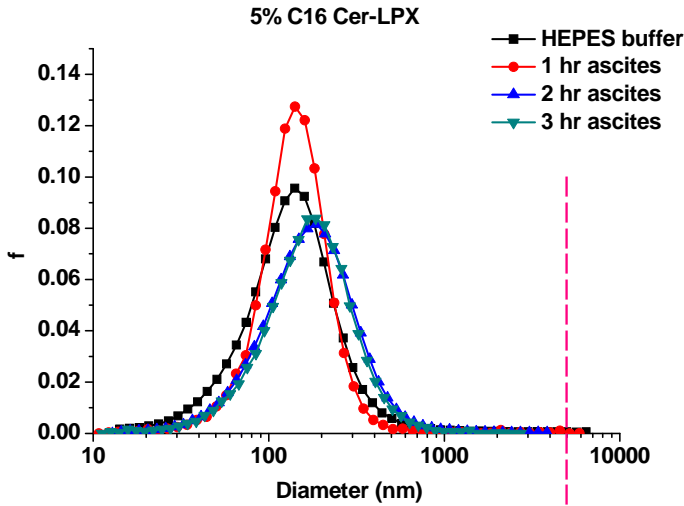
Figure 2. Complexation efficiency of liposomes immediately following preparation in HEPES buffer (grey bars) and percentage of siRNA still complexed after incubation of the lipoplexes in 90 vol% of human ascites fluid during respectively 1 h (white bars) and 24 h (dark grey bars).

Figure 3

a)



b)



c)

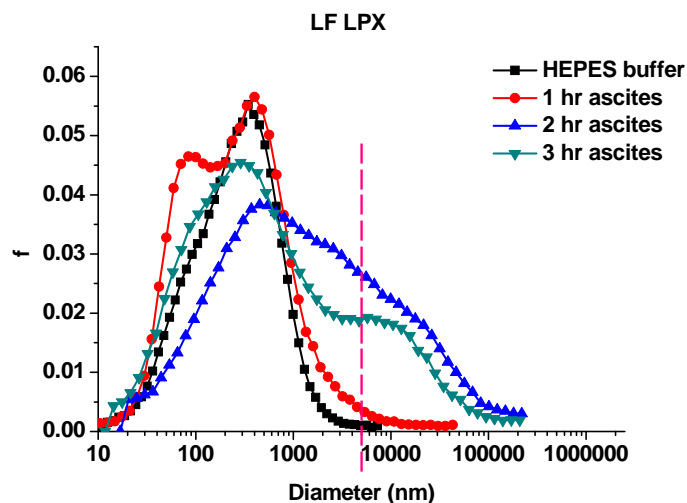
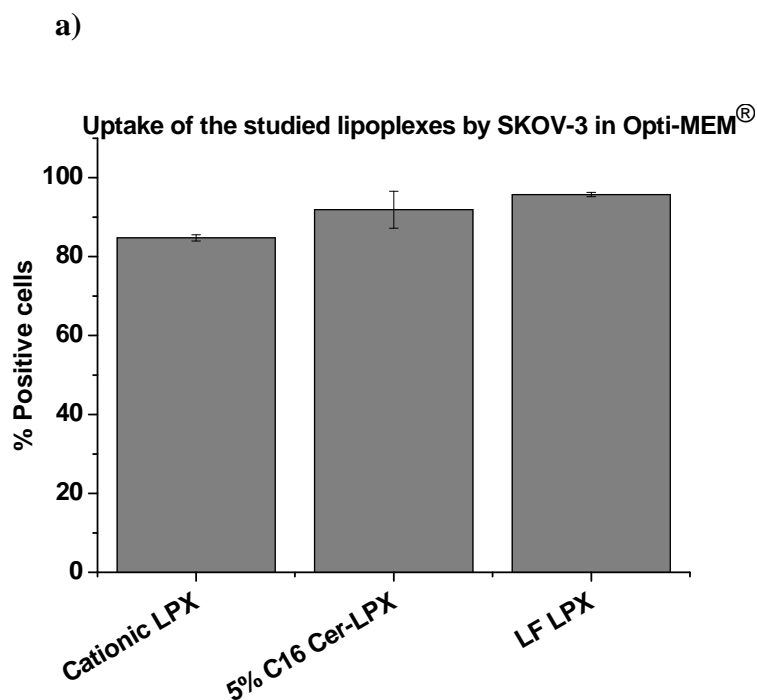


Figure 3. fSPT size distributions of the different lipoplexes following incubation in 90 vol% human ascites fluid at 37°C. (a) cationic LPXs, (b) 5% C16 Cer-LPXs and (c) LF-LPXs. The dotted (pink) line corresponds to 5 μm in size aggregates. The Y-axis refers to the fraction (f) of nanoparticles that appear with the corresponding size on the X-axis.

Figure 4



b)

Uptake of the studied lipoplexes following incubation in ascites fluid

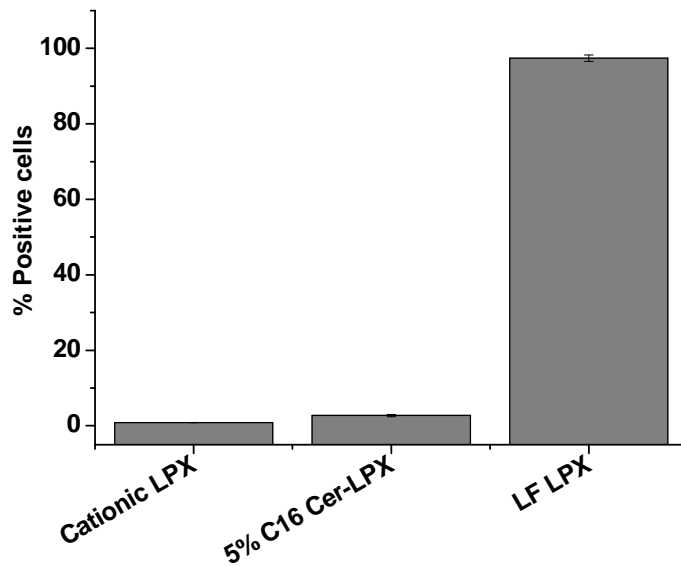


Figure 4. Uptake of AF-488 siRNA labeled lipoplexes by SKOV-3 cells. Lipoplexes were prepared in HEPES buffer and added to the cells in Opti-MEM® following preparation as such (a) or after incubation of the lipoplexes for 1 h in human ascites fluid before adding them on the cells (b).

Figure 5

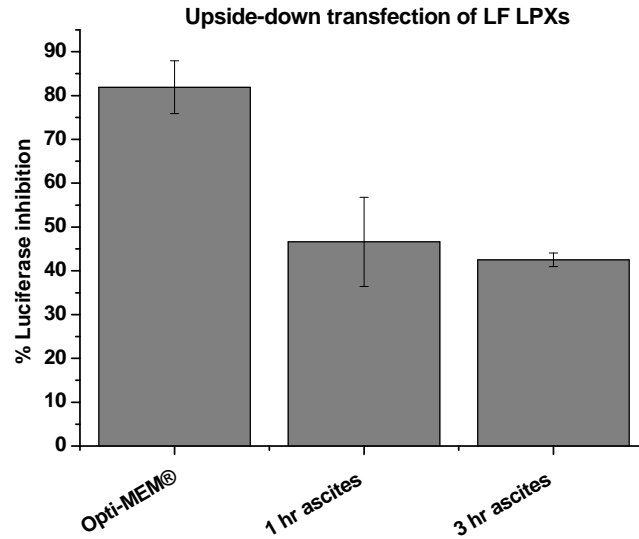


Figure 5. Luciferase inhibition, following upside-down transfections, by LF-LPXs, respectively in Opti-MEM® and following incubation of the complexes for 1 h and 3 h in ascites fluid. The values in the graph represent the average from at least 3 experiments that were performed on different days.

Liposomal formulations

